This is a preprint, the final version is subject to change, of the American Mineralogist (MSA)
Cite as Authors (Year) Title. American Mineralogist, in press.
DOI: https://doi.org/10.2138/am-2020-7308

First-Principles Modeling of X-Ray Absorption Spectra Enlightens the Processes of Scandium Sequestration by Iron Oxides

REVISION 1

Mathieu CHASSÉ[1,*], Marc BLANCHARD[2], Delphine CABARET[1], Amélie JUHIN[1], Delphine VANTELON[3] & Georges CALAS[1]

[1]Sorbonne Université, Muséum National d'Histoire Naturelle, UMR CNRS 7590, IRD, Institut de minéralogie, de physique des matériaux et de cosmochimie, IMPMC, 75005 Paris, France

[2]Géosciences Environnement Toulouse (GET), Observatoire Midi-Pyrénées, Université de Toulouse, CNRS, IRD, UPS, 14 avenue Edouard Belin, 31400 Toulouse, France

[3]SOLEIL synchrotron, L'Orme des Merisiers, Saint-Aubin, BP 48, 91192 Gif-sur-Yvette, France

[*]Corresponding author: mathieu.chasse@normalesup.org

Abstract

Scandium is often associated with iron oxides in the environment. Despite the use of scandium as a geochemical tracer and the existence of world-class supergene deposits, uncertainties on speciation obscure the processes governing its sequestration and concentration. Here, we use first-principles approaches to interpret experimental *K*-edge X-ray absorption near-edge structure spectra of scandium either incorporated in or adsorbed on goethite and hematite, at concentrations relevant for the environment. This modeling helps to interpret the characteristic spectral features, providing key information to determine scandium speciation when associated with iron oxides. We show that scandium is substituted into iron oxides at low concentration without modifying the crystal structure.

Always consult and cite the final, published document. See http:/www.minsocam.org or GeoscienceWorld

When scandium is adsorbed onto iron oxide surfaces, the process occurs through outer-sphere complexation with a reduction in the coordination number of the hydration shell. Considering available X-ray absorption spectra from laterites, the present results confirm that scandium adsorption onto iron oxides is the dominant mechanism of sequestration in these geochemical conditions. This speciation explains efficient scandium recovery through mild metallurgical treatments of supergene lateritic ores. The specificities of scandium sorption mechanisms are related to the preservation of adsorbed scandium in million-years old laterites. These results demonstrate the emerging ability to precisely model fine X-ray absorption spectral features of trace metals associated with mineral phases relevant to the environment. It opens new perspectives to accurately determine trace metals speciation from high-resolution spatially-resolved X-ray absorption near-edge structure spectroscopy in order to constrain the molecular mechanisms controlling their dynamics.

Keywords: Scandium, XANES, Ab-Initio Calculations, Speciation, Fe oxides, Sorption, Critical Zone.

Introduction

In the critical zone (CZ: the interface between geological, hydrological and atmospheric compartments where rocks interact with air, water and biota), iron oxides, in particular goethite (α–FeO(OH)) and hematite (α–Fe_2O_3), are ubiquitous. They affect the biogeochemical cycling of many elements as they bind through adsorption onto mineral surfaces or incorporate within the crystal structure (Brown and Calas, 2012). Adsorption can also be followed by diffusive penetration into the interior of mineral particles through lattice or pore diffusion (Brümmer et al. 2013). Recurring changes of the biogeochemical conditions within the CZ lead to dynamic dissolution and crystallization of Fe oxides controlling the fate of trace metals (e.g., Frierdich et al., 2011).

The fate of scandium (Sc) in the CZ is a case in point. Scandium is used as a conservative element to model mass transfer during weathering (e.g., Eshel et al., 2015). The absence of accessory Sc minerals

in supergene contexts (Samson and Chassé 2016) implies that its sequestration in the CZ depends on the rock-forming phases present. Scandium association with Fe oxides is well-known (Norman and Haskin 1968) and illustrated by worldwide findings of Sc-rich laterites (e.g., Aiglsperger et al., 2016; Chassé et al., 2017; Teitler et al., 2019), expected to become a potential source for this critical metal. Nonetheless, the processes of Sc trapping in laterites remain elusive. Isomorphous substitution in Fe oxides or sequestration by adsorption have been invoked in Sc-bearing laterites (Chassé et al. 2017; Vind et al., 2018; Ulrich et al., 2019), making necessary an accurate determination of Sc speciation to constrain Sc dynamics in the CZ.

In this perspective, the chemical selectivity and high sensitivity of X-ray absorption spectroscopy proved to be invaluable (Chassé et al. 2017, 2019). The low Sc concentration in natural systems requires the use of Sc *K*-edge X-ray absorption near-edge structure (XANES) spectroscopy. Nonetheless, a precise analysis of Sc speciation based on XANES spectroscopy requires theoretical modeling to understand the origin of the spectral features. This has been made for the first time on the Sc *K*-edge XANES spectra of mineral compounds using first-principles calculations (Chassé et al., 2018). We apply this density functional theory (DFT) approach to model XANES spectra of Sc trapped by Fe oxides, stressing the interest of the method to unravel the role of incorporation and sorption processes on Sc fate in the CZ.

Experimental methods and theoretical approach

We studied a Sc-chloride solution (ca. 1 wt%), Sc-substituted (ca. 1 wt%) and Sc-adsorbed (ca. 0.1 wt %) goethite and hematite, and Sc-adsorbed montmorillonite ($(Na,Ca)_{0.3}(Al,Mg)_2Si_4O_{10}(OH)_2 \cdot nH_2O$, ca. 1 wt%). The Sc-chloride solution was prepared by dilution of Sc^{3+} chloride hexahydrate powder. Scandium-substituted goethite was prepared by maintaining a ferrihydrite suspension at 65 °C for two days after precipitation from Fe^{3+} nitrate at a basic pH in presence of Sc chloride. Scandium-substituted

This is a preprint, the final version is subject to change, of the American Mineralogist (MSA)
Cite as Authors (Year) Title. American Mineralogist, in press.
DOI: https://doi.org/10.2138/am-2020-7308

hematite was obtained by dehydroxylation of goethite through heating. Scandium-adsorbed samples were prepared by adding a Sc-chloride solution to Sc-free synthetic goethite, hematite or natural montmorillonite, later separated and dried. Details are given in Supplemental Material.

We recorded Sc *K*-edge XANES spectra at the LUCIA beamline (SOLEIL synchrotron) using an Si(311) double crystal monochromator calibrated against a Sc_2O_3 standard. Measurements were performed in the energy range (4400–4800) eV with energy steps of (5, 0.2, 0.5 and 1) eV in energy ranges of (4400–4485) eV, (4485–4534) eV, (4534–4586) eV and (4586–4800) eV, respectively. Spectra were collected at room temperature, under vacuum in XRF mode on pellets obtained from powdered material and mounted on a holder between two 2 μm thick Ultralene® films, using a four-element silicon drift detector (SDD). Two spectra were recorded for each reference with a counting time of ca. 50 s per spectrum. The spectra acquired for each reference were merged before background subtraction and normalization. Details can be found in Chassé et al. (2017).

Theoretical XANES spectra were calculated using the Quantum ESPRESSO plane-wave based DFT suite of codes (Giannozzi et al. 2009) in the generalized gradient approximation (Perdew–Burke–Ernzerhof parametrization, Perdew et al., 1996). The charge density is obtained via a relaxation of the atomic positions and a self-consistent field calculation using the PWscf code. Then, XANES spectra are computed in a continued fraction approach using the XSpectra code (Taillefumier et al. 2002; Gougoussis et al. 2009). Computational details are given in Supplemental Material.

Charge density calculations were initialized using cell parameters and atomic positions obtained from structure relaxations of goethite (Ducher et al. 2015) and hematite (Blanchard et al. 2008). Either one or two adjacent Sc atoms (isolated or paired models, Supplemental Material) were substituted for Fe atoms into the crystal structure to model Sc-substituted goethite (Fig. 1a) and hematite (Fig. 1b). It corresponds to ca. 2 wt% and 4 wt% Sc for goethite models and ca. 1 wt% and 2 wt% Sc for hematite models. Physiosorbed Sc was modeled by a 6-fold coordinated water complex (Rudolph and Pye

Always consult and cite the final, published document. See http:/www.minsocam.org or GeoscienceWorld

2000).

Results and discussion

Spectral signature of scandium associated with iron oxides

Experimental Sc *K*-edge XANES spectra of Sc-substituted goethite and hematite exhibit four major features in the main edge (A_0, A, B and C, Fig. 2a,b), respectively located at ca. 4501 eV, 4508 eV, 4512 eV and 4524 eV. In the pre-edge region, two low-intensity features (P_1 and P_2), observed in compounds with six-fold coordinated Sc (Lindqvist-Reis et al. 2006; Oberti et al. 2006; Chassé et al. 2018), are present at ca. 4492 eV and 4494 eV. The position, shape and intensity of the main-edge features are reproduced in the theoretical spectra obtained from structural models of Sc-incorporated goethite and hematite indicating the robustness of the calculation method and the validity of the structural models (Fig. 2a,b). In the pre-edge region, the P_2 feature is less intense and split in two components in the theoretical spectra (close view, Figs. 3 and S1). When Sc atoms are paired in the model structure of goethite, a feature appears at higher energy (Fig. 3, *).

To interpret the pre-edge spectra, the DOS, correlated to the spectral features, are projected on the absorbing Sc (Sc*) and its first neighbors (Fig. 3 and S1). These DOS describe, for each energy level, the number of empty states available that can be reached with a certain transition probability by the photoelectron during XANES experiments. The contribution of electric quadrupole (E2) transitions to the P_1 and P_2 features, corresponding respectively to $1s \rightarrow 3d–t_{2g}$ and $1s \rightarrow 3d–e_g$ transitions is minor (Figs. 3 and S1). Electric dipole (E1) transitions $1s \rightarrow 4p$ dominate the P features. They reflect local transitions due to $4p–3d$ hybridization of Sc*, observed for non-centrosymmetric sites, such as tetrahedra (Knoll et al. 2014) or distorted octahedra (Chassé et al. 2018). Non-local transitions also contribute to E1 transitions and result from orbital mixing between the 4*p* orbitals of Sc* and 3*d* orbitals of its nearest Fe neighbors *via* the empty 2*p* orbitals of the oxygen ligands. This orbital mixing of Sc* is documented for Sc-bearing compounds exhibiting 3*d* neighbors (Chassé et al. 2018). The

DOS show that the energy difference between 3*d*–t_{2g} and 3*d*–e_g orbitals, i.e. the crystal field splitting energy (10Dq), is greater for Sc than for Fe, inducing the splitting of the P_2 feature. The 10Dq value for Fe tends to be underestimated compared to experiments (Ducher et al. 2016). A higher 10Dq would lead to the superimposition of the theoretical P_2 features, matching experimental spectra. When Sc atoms are paired in the model structure of goethite and hematite, non-local E1 transitions may also arise from orbital mixing with 3*d* orbitals of the adjacent Sc ions. Due to the absence of core hole on these neighbors, the position of the 3*d* orbitals is at higher energies, leading to additional features on the calculated pre-edge (Figs. 3 and S1, shown as *, at ca. 4497 eV for goethite and at ca. 4496 eV and 4498 eV for hematite), absent from experimental spectra. This additional feature is unambiguous in the hematite spectrum when plotting the different polarization dependent components of the isotropic spectrum (Fig. S2). Such additional pre-edge features are also observed for Sc oxides (Chassé et al. 2018) and for other 3*d* ions in oxides such as Ti^{4+} (Cabaret et al. 2010) and Cr^{3+} ions (Verger et al. 2016) accounting for the presence of neighbors with the same nature as the absorbing atom.

Atomic environment of scandium associated to iron oxides

The agreement between experimental and theoretical spectra in the main edge confirms the structural incorporation of Sc in the synthesized Fe oxides. Despite small discrepancies in the energy and intensity of some transitions, inherent to the limitation of DFT-based methods to model the core–hole electron interaction and the 3*d* electron–electron repulsion (Cabaret et al. 2010), the transitions observed in the pre-edge are reproduced and interpreted from the projected DOS. The absence of the feature diagnostic of Sc pairing (Figs. 3 and S1, *) in experimental spectra of goethite and hematite indicates that substituted Sc sites are isolated. A correct modeling of the spectra does not require volume-cell relaxation. At low Sc concentrations, below a few wt%, the structure of these Fe oxides accommodates Sc substitution without significant changes in the cell volume, the changes in Sc–O

This is a preprint, the final version is subject to change, of the American Mineralogist (MSA)
Cite as Authors (Year) Title. American Mineralogist, in press.
DOI: https://doi.org/10.2138/am-2020-7308

distances relative to Fe–O distances remaining low (< 7 %, Supplemental Table S1). When Sc is structurally incorporated, it is dispersed at low concentration, without modifying the Fe-oxides cell volume.

Scandium *K*-edge XANES spectra of Sc-adsorbed goethite and hematite are similar and alike that of Sc adsorbed on Fe-free clay surfaces (Fig. 2c). Specific affinity for a given site of Fe-oxide surfaces and adsorption through covalent bonding is thus excluded. Scandium binding must occur through outer sphere complexes. Comparison with such Sc complexes indicates that the splitting of the pre-edge associated with the low intensity of the main edge is consistent with six-fold coordinated complexes but incompatible with higher coordination numbers (Fig. 2c, Sc-chloride solution and Lindqvist-Reis et al., 2006; Yamaguchi et al., 1997). A theoretical spectrum is calculated using an isolated 6-fold coordinated $[Sc(H_2O)_4(OH)_2]^+$ complex, $Sc(OH)_2^+$ being the dominant species at the slightly acidic pH of adsorption experiments (Wood and Samson 2006). The calculated spectrum reproduces the major features exhibited by experimental spectra (A and B, Fig. 2c). The splitting of the pre-edge and the relative intensity of the two features is reproduced (P_1 and P_2, Fig. 2c). Despite discrepancies in this region arising from the simpleness of the model, the closeness between the calculated spectrum and the experimental spectra of adsorbed Sc indicates that adsorption results in a reduction of the coordination number of the Sc^{3+} complex. This complex is seven- to nine-fold coordinated in solution (Vchirawongkwin et al. 2012, illustrated by the spectrum of the Sc-chloride solution, Fig. 2c) and six-fold coordinated at the surface of Fe oxides (illustrated by the spectrum of Sc-adsorbed goethite and hematite, Fig. 2c). The lability of the Sc^{3+} hydration shell supports this observation (Migliorati and D'Angelo 2016).

Mechanisms of scandium sequestration by iron oxides in the critical zone

First-principles calculations do not show significant difference of affinity for Sc substitution in goethite

Always consult and cite the final, published document. See http:/www.minsocam.org or GeoscienceWorld

or hematite ($\Delta E_{Gt–Hem}$ = 0.33 eV, Supplemental Material and Table S2). Preferential incorporation into goethite (Ulrich et al. 2019) or hematite (Vind et al., 2018) must reflect the role of the conditions of formation in determining the nature of the phase incorporating Sc, as shown for lutetium (Yokosawa et al. 2019). In particular, differences in specific surface area or distinct precursor phases during Fe oxides crystallization can explain variations in affinity for Sc. Sorption to goethite in lateritic Fe oxide-rich horizons plays a major role in Sc trapping and concentration processes (Chassé et al. 2019). The theoretical modeling of the spectra of outer-sphere Sc complexes exhibit features for which the position, intensity and shape are comparable to experimental spectra of Sc-adsorbed species and bulk lateritic samples (Fig. 2c). The agreement with experimental spectra of Sc-substituted goethite and hematite excludes trapping by structural incorporation within crystallized Fe oxides in supergene contexts, despite the existence of a solid solution $Fe_xSc_{(1–x)}O(OH)$ in mild hydrothermal conditions (70 °C, Levard et al., 2018). Subtle differences between spectra of lateritic samples and Sc-adsorbed Fe oxides (Fig. 2c, +), close to major features observed in Sc-substituted reference spectra, indicate minor incorporation. With aging, as other metallic ions (Brümmer et al., 2013), Sc could penetrate Fe oxides following adsorption processes enhanced by nanoporosity or lattice diffusion. The physico-chemical parameters and growth kinetics are key determinants of the mechanism of Sc sorption. At increasing metal concentration in solution, the process of adsorption through complexation at goethite surface may be replaced by the formation of surface precipitates and structural incorporation, such as is the case for nickel (Ugwu et al. 2019). At environmental conditions, with low Sc concentrations (< a few tenth of wt%) and room temperature (ca. 30 °C on average under tropical climates), the surface complexation process and slow kinetics must favor Sc adsorption onto goethite at the expense of structural incorporation. In particular, the kinetics of this process in competition with successive dissolution and crystallization processes may lead to the preservation of Sc complexes during the formation and evolution of lateritic profiles.

Implications

A speciation explaining mineral processing results. The speciation of critical metals has direct implications for ore processing. For instance, cobalt sorption to goethite is mainly irreversible when forming monodentate complexes while leaching remains efficient when polydentate polynuclear complexes form (Ugwu and Sherman, 2017). The preservation of Sc sorbed onto Fe oxides surfaces in laterites explains why Sc is efficiently recovered from lateritic ores using ion exchange (79 % recovery, Williams-Jones and Vasyukova, 2018) or high-pressure acid leaching processes (94 % recovery with limited Fe-oxides dissolution, Wang et al., 2011).

An original sorption process controlling Sc fate in the critical zone. The nature of the adsorption process may be of importance to the stability of Sc sorption after aging. The exchange of water molecules inside the solvation shell of Sc with the solvent is eased by the existence of a far-coordinated water molecule capping the complex (Migliorati and D'Angelo 2016), facilitating geometric changes required for Sc adsorption and stabilizing the six-fold coordinated complex. The persistence of adsorbed Sc species in million-years old laterites may result from this original sorption mechanism.

A promising tool to study the speciation of trace metals in the critical zone. This study demonstrates that state-of-the-art first-principles calculations can reproduce XANES spectra of metals associated with phases ubiquitous in the CZ. The complexity of the pathways leading to Sc trapping in the CZ and their dependence to varying environmental conditions are evidenced. As for other trace metals, experimental sequestration on model systems prepared in diverse but controlled conditions are required as references to determine speciation in natural contexts. This theoretical tool, combined to XANES, offers a new opportunity to make the link between experiments and natural environments to obtain direct information on the molecular environment of trapping at trace concentration.

Future directions for first-principles-assisted investigation in environmental mineralogy. X-ray

absorption spectroscopy has become a central tool in environmental sciences (Brown and Calas 2012). In the case of transition elements, the pre-edge features are used to determine element speciation but their understanding is still complicated by the limitation of DFT-based approaches in this region. A better modeling of the core-hole effects and of electron-electron interactions in DFT-based software is developed (e.g., Cabaret et al. 2010) and will further improve the agreement between experimental and calculated pre-edge spectra. Another direction, specific to adsorbed elements, would be to combine DFT-based calculations of X-ray absorption spectra with DFT-based molecular dynamic simulations to determine the molecular environments of adsorption and their energies (e.g., Watts et al. 2019).

Acknowledgements

We thank Benoît Baptiste, Ludovic Delbes and the late Jean-Louis Robert for experimental support. We acknowledge SOLEIL for provision of synchrotron radiation facilities and thank the staff of the LUCIA beamline (Proposal No. 20150692). Computer facilities were provided by GENCI–IDRIS (Projects Nos. A0020906863 and A0040906863). This work was funded by the Institut universitaire de France.

References

Aiglsperger, T., Proenza, J.A., Lewis, J.F., Labrador, M., Svojtka, M., Rojas-Purón, A., Longo, F. and Durišová, J. (2016) Critical metals (REE, Sc, PGE) in Ni laterites from Cuba and the Dominican Republic. Ore Geology Reviews, 73, 127–147.

Blanchard, M., Lazzeri, M., Mauri, F. and Balan, É. (2008) First-Principles Calculation of the Infrared Spectrum of Hematite. American Mineralogist, 93, 1019–1027.

Brown Jr. G.E. and Calas G. (2012) Mineral–Aqueous Solution Interfaces and Their Impact on the Environment. Geochemical Perspectives, 1, 483–742.

Brümmer, G.W., Barrow, N.J. and Fischer, L. (2013) Effect of Porosity of Goethite on the Sorption of Six Heavy Metal Ions: Sorption of Metals by Different Goethites. European Journal of Soil Science,

64, 805–813.

Cabaret, D., Bordage, A., Juhin, A., Arfaoui, M., and Gaudry, E. (2010) First-Principles Calculations of X-Ray Absorption Spectra at the *K*-Edge of 3*d* Transition Metals: an Electronic Structure Analysis of the Pre-Edge. Physical Chemistry Chemical Physics, 12, 5619–5633.

Chassé, M., Griffin, W.L., O'Reilly, S.Y. and Calas, G. (2017) Scandium Speciation in a World-Class Lateritic Deposit. Geochemical Perspectives Letters, 3, 105-114.

Chassé, M., Juhin, A., Cabaret, D., Delhommaye, S., Vantelon, D. and Calas, G. (2018) Influence of Crystallographic Environment on Scandium *K*-Edge X-Ray Absorption Near-Edge Structure Spectra. Physical Chemistry Chemical Physics, 20, 23903.

Chassé, M., Griffin, W.L., O'Reilly, S.Y. and Calas, G. (2019) Australian Laterites Reveal Mechanisms Governing Scandium Dynamics in the Critical Zone. Geochimica Cosmochimica Acta, 260, 292–310.

Ducher, M., Blanchard, M., Vantelon, D., Nemausat, R. and Cabaret, D. (2016) Probing the Local Environment of Substitutional Al^{3+} in Goethite Using X-Ray Absorption Spectroscopy and First-Principles Calculations. Physics and Chemistry of Minerals, 43, 1-11.

Eshel, G., Lin, C. and Banin, A. (2015) Novel Approach for Quantitatively Estimating Element Retention and Material Balances in Soil Profiles of Recharge Basins Used for Wastewater Reclamation. Science of the Total Environment, 502, 517-525.

Frierdich, A.J., Luo, Y. and Catalano, J.G. (2011) Trace Element Cycling Through Iron Oxide Minerals During Redox-Driven Dynamic Recrystallization. Geology, 39, 1083–1086.

Giannozzi, P., Baroni, S., Bonini, N., Calandra, M., Car, R., Cavazzoni, C., Ceresoli, D., Chiarotti, G.L., Cococcioni, M., Dabo, I., Dal Corso, A., De Gironcoli, S., Fabris, S., Fratesi, G., Gebauer, R., Gerstmann, U., Gougoussis, C., Kokalj, A., Lazzeri, M., Martin-Samos, L., Marzari, N., Mauri, F., Mazzarello, R., Paolini, S., Pasquarello, A., Paulatto, L., Sbraccia, C., Scandolo, S., Sclauzero, G., Seitsonen, A.P., Smogunov, A., Umari, P. and Wentzcovitch, R.M. (2009) QUANTUM ESPRESSO: A Modular and Open-Source Software Project for Quantum Simulations of Materials. Journal of Physics: Condensed Matter, 21, 395502.

Gougoussis, C., Calandra, M., Seitsonen, A.P. and Mauri, F. (2009) First-Principles Calculations of X-Ray Absorption in a Scheme Based on Ultrasoft Pseudopotentials: From α-Quartz to High-T_c Compounds. Physical Review B, 80, 1-8.

Knoll, S.M., Rovezzi, M., Zhang, S., Joyce, T.B., and Moram, M.A. (2014) Electronic Structure and Local Distortions in Epitaxial ScGaN Films. Journal of Physics: Condensed Matter, 26, 225801.

Levard, C., Borschneck, D., Grauby, O., Rose, J. and Ambrosi, J.-P. (2018) Goethite, a Tailor-Made Host for the Critical Metal Scandium: The $Fe_xSc_{(1-x)}OOH$ solid solution. Geochemical Perspectives

This is a preprint, the final version is subject to change, of the American Mineralogist (MSA)
Cite as Authors (Year) Title. American Mineralogist, in press.
DOI: https://doi.org/10.2138/am-2020-7308

Letters, 9, 16-20.

Lindqvist-Reis, P., Persson, I. and Sandström, M. (2006) The Hydration of the Scandium(III) Ion in Aqueous Solution and Crystalline Hydrates Studied by XAFS Spectroscopy, Large-Angle X-Ray Scattering and Crystallography. Dalton Transactions, 32, 3868-3878.

Migliorati, V. and D'Angelo, P. (2016) Unraveling the Sc^{3+} Hydration Geometry: The Strange Case of the Far-Coordinated Water Molecule. Inorganic Chemistry, 55, 6703-6711.

Norman, J.C. and Haskin, L.A. (1968) The Geochemistry of Sc: A Comparison to the Rare Earths and Fe. Geochimica Cosmochimica Acta, 32, 93–108.

Oberti, R., Quartieri, S., Dalconi, M.C., Boscherini, F., Iezzi, G., Boiocchi, M., and Eeckhout, S.G. (2006) Site Preference and Local Geometry of Sc in Garnets: Part I. Multifarious Mechanisms in the Pyrope--Grossular Join. American Mineralogist, 91, 1230–1239.

Perdew, J. P., Burke, K. and Ernzerhof, M. (1996) Generalized Gradient Approximation Made Simple. Physical Review Letters, 77, 3865-3868.

Rudolph, W.W. and Pye, C.C. (2000) Raman Spectroscopic Measurements of Scandium(III) Hydration in Aqueous Perchlorate Solution and Ab Initio Molecular Orbital Studies of Scandium(III) Water Clusters: Does Sc(III) Occur as a Hexaaqua Complex? The Journal of Physical Chemistry A, 104, 1627-1639.

Samson, I.M. and Chassé, M. (2016) Scandium. In W.M. White, Ed., Encyclopedia of Geochemistry, p. 1-5. Springer International Publishing, Cham.

Taillefumier, M., Cabaret, D., Flank, A.-M. and Mauri, F. (2002) X-ray Absorption Near-Edge Structure Calculations with the Pseudopotentials: Application to the *K*-edge in Diamond and α-Quartz. Physical Review B, 66, 195107.

Teitler, Y., Cathelineau, M., Ulrich, M., Ambrosi, J.-P., Muñoz, M. and Sevin, B. (2019) Petrology and Geochemistry of Scandium in New Caledonian Ni-Co Laterites. Journal of Geochemical Exploration, 196, 131-155.

Ugwu, I.M. and Sherman, D.M. (2017) Irreversibility of Sorption of Cobalt to Goethite (α-FeOOH) and Disparities in Dissolution of Aged Synthetic Co-Goethite. Chemical Geology, 467, 168–176.

Ugwu, I.M., Sherman, D.M. and Bacon, C.G.D. (2019) Sorption of Nickel Onto Goethite (α-FeOOH) and Desorption Kinetics of Aged Synthetic Ni-Goethite: Implication for Ni Laterite Ore. Chemical Geology, 509, 223–233.

Ulrich, M., Cathelineau, M., Muñoz, M., Boiron, M.-C., Teitler, Y. and Karpoff, A.-M. (2019) The Relative Distribution of Critical (Sc, REE) and Transition Metals (Ni, Co, Cr, Mn, V) in Some Ni-Laterite Deposits of New Caledonia. Journal of Geochemical Exploration, 197, 93-113.

Always consult and cite the final, published document. See http:/www.minsocam.org or GeoscienceWorld

Vchirawongkwin, V., Kritayakornupong, C., Tongraar, A. and Rode, B.M. (2012) Characterization of Structure and Dynamics of an Aqueous Scandium(III) Ion by an Extended Ab Initio QM/MM Molecular Dynamics Simulation. Dalton Transactions, 41, 11889.

Verger, L., Dargaud, O., Rousse, G., Rozsályi, E., Juhin, A., Cabaret, D., Cotte, M., Glatzel, P., and Cormier, L. (2016) Spectroscopic properties of Cr^{3+} in the spinel solid solution $ZnAl_{2-x}Cr_xO_4$. Physics and Chemistry of Minerals, 43, 33–42.

Vind, J., Malfliet, A., Bonomi, C., Paiste, P., Sajó, I.E., Blanpain, B., Tkaczyk, A.H., Vassiliadou, V. and Panias, D. (2018) Modes of Occurrences of Scandium in Greek Bauxite and Bauxite Residue. Mineral Engineering, 123, 35-48.

Wang, W., Pranolo, Y. and Cheng, C.Y. (2011) Metallurgical Processes for Scandium Recovery from Various Resources: a Review. Hydrometallurgy, 108, 100-108.

Watts, H.D., O'Day, P.A., and Kubicki, J.D. (2019) Gibbsite (100) and Kaolinite (100) Sorption of Cadmium(II): A Density Functional Theory and XANES Study of Structures and Energies. The Journal of Physical Chemistry A, 123, 6319–6333.

Williams-Jones, A.E. and Vasyukova, O.V. (2018) The Economic Geology of Scandium, the Runt of the Rare Earth Element Litter. Economic Geology, 113, 973-988.

Wood, S.A. and Samson, I.M. (2006) The Aqueous Geochemistry of Gallium, Germanium, Indium and Scandium. Ore Geology Reviews, 28, 57-102.

Yamaguchi, T., Niihara, M., Takamuku, T., Wakita, H. and Kanno, H. (1997) Scandium(III) hydration in aqueous solution from X-ray diffraction and X-ray absorption fine structure measurements. Chemical Physics Letters, 274, 485–490.

Yokosawa, T., Prestat, E., Polly, R., Bouby, M., Dardenne, K., Finck, N., Haigh, S.J., Denecke, M.A. and Geckeis, H. (2019) Fate of Lu(III) Sorbed on 2-Line Ferrihydrite at pH 5.7 and Aged for 12 Years at Room Temperature. II: Insights from STEM-EDXS and DFT Calculations. Environmental Science and Pollution Research, 26, 5282-5293.

This is a preprint, the final version is subject to change, of the American Mineralogist (MSA)
Cite as Authors (Year) Title. American Mineralogist, in press.
DOI: https://doi.org/10.2138/am-2020-7308

337

338

339 **List of figures**

340 **Figure 1** Representations of the supercells of Sc-substituted goethite (2 × 1 × 3) **(a)** and hematite
341 (2 × 2 × 1) **(b)**, and of the $[Sc(H_2O)_4(OH)_2]^+$ model complex **(c)** considered in the present study. The
342 two-tone sites can either be occupied by Fe (isolated model) or by Sc (paired model).

343 **Figure 2** Comparison between experimental (red) and calculated (black) normalized Sc *K*-edge
344 XANES spectra for Sc-substituted goethite **(a)** and hematite **(b)** and Sc-adsorbed goethite and hematite
345 **(c)**. Additional reference spectra of a $ScCl_3$ solution (ca. 1 wt% Sc), Sc-adsorbed montmorillonite
346 (ca. 1 wt% Sc) and from a lateritic sample (ca. 750 ppm Sc, Chassé et al. 2017) are given for
347 comparison in **(c)**. Calculated spectra are shifted in energy to match the experimental A feature. The
348 symbols + indicate features discussed in the paper.

349 **Figure 3** Experimental and calculated pre-edge regions of Sc *K*-edge XANES spectra of Sc-substituted
350 goethite: **(a)** isolated structural model; **(b)** paired structural model. The calculated electric dipole (E1)
351 and quadrupole (E2) contributions are displayed. The partial densities of the absorbing Sc (Sc*) 4*p* and
352 3*d* states, of the first six O neighbors 2*p* states, of the first Fe and Sc neighbors 3*d* states are shown.
353 The energy scale of the experimental spectra is shifted to match calculated spectra. The vertical line
354 indicates the Fermi level (E_F). The * symbol indicate features discussed in the paper.

Always consult and cite the final, published document. See http:/www.minsocam.org or GeoscienceWorld

This is a preprint, the final version is subject to change, of the American Mineralogist (MSA)
Cite as Authors (Year) Title. American Mineralogist, in press.
DOI: https://doi.org/10.2138/am-2020-7308

Feuille1

			Goethite
	Interatomic distances (Å)		
Oxygen neighbor	Fe–O	Sc–O (isolated)	Difference relative to Fe–O distances (%)
O1	1.90	2.03	6.84
O2	1.98	2.07	4.55
O3	1.98	2.07	4.55
O4	2.12	2.16	1.89
O5	2.12	2.16	1.89
O6	2.14	2.15	0.47
			Hematite
	Interatomic distances (Å)		
Oxygen neighbor	Fe–O	Sc–O (isolated)	Difference relative to Fe–O distances (%)
O1	1.93	2.04	5.70
O2	1.93	2.04	5.70
O3	1.93	2.04	5.70
O4	2.14	2.17	1.40
O5	2.14	2.17	1.40
O6	2.14	2.17	1.40

Table S1

Always consult and cite the final, published document. See http:/www.minsocam.org or GeoscienceWorld

This is a preprint, the final version is subject to change, of the American Mineralogist (MSA)
Cite as Authors (Year) Title. American Mineralogist, in press.
DOI: https://doi.org/10.2138/am-2020-7308

Sc–O (paired)	Difference relative to Fe–O distances (%)
2.03	6.40
2.04	2.94
2.08	4.81
2.16	1.85
2.16	1.85
2.15	0.47

Sc–O (paired)	Difference relative to Fe–O distances (%)
2.03	5.18
2.03	5.18
2.03	5.18
2.19	2.34
2.19	2.34
2.19	2.34

Always consult and cite the final, published document. See http:/www.minsocam.org or GeoscienceWorld

This is a preprint, the final version is subject to change, of the American Mineralogist (MSA)
Cite as Authors (Year) Title. American Mineralogist, in press.
DOI: https://doi.org/10.2138/am-2020-7308

Total energy (eV)		
Goethite	Sc-substituted goethite (isolated)	Sc-substituted goethite (paired)
39459.87	40037.77	40615.77
Hematite	Sc-substituted hematite (isolated)	Sc–substituted hematite (paired)
67718.57	68296.14	68873.69

Table S2

Always consult and cite the final, published document. See http:/www.minsocam.org or GeoscienceWorld

Figure 1

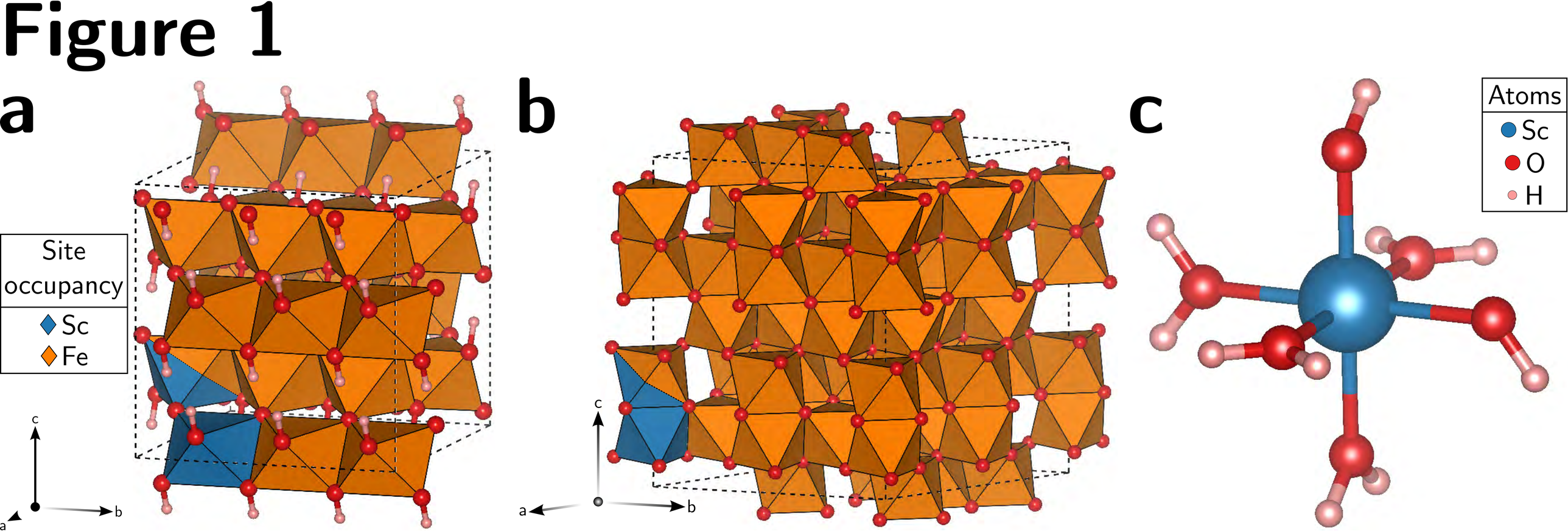

Figure 2

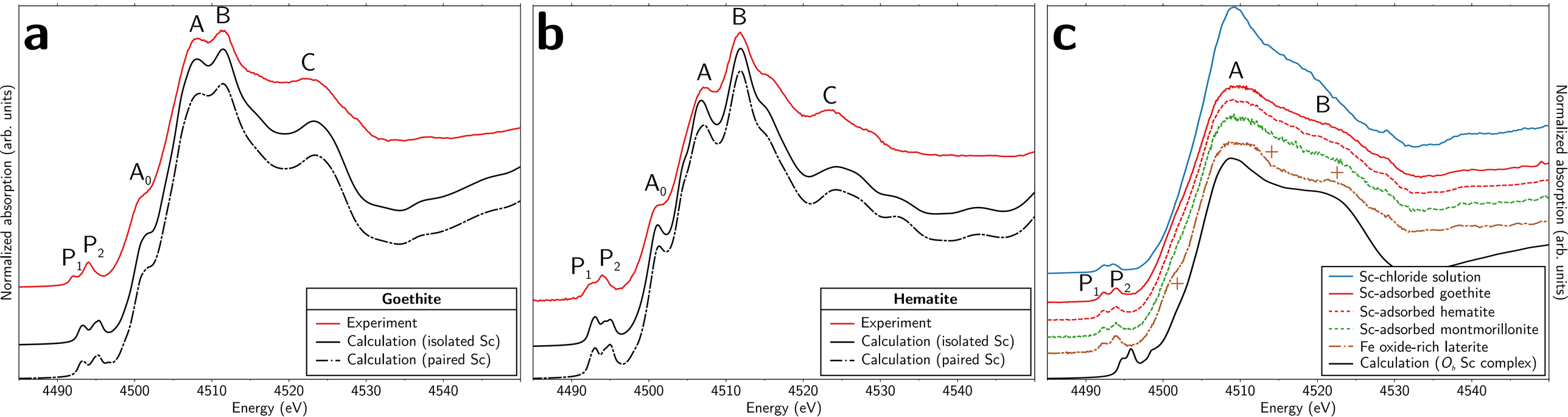
a
b
c
A
B
C
A0
P1
P2
Normalized absorption (arb. units)
Energy (eV)
4490
4500
4510
4520
4530
4540
Goethite
Experiment
Calculation (isolated Sc)
Calculation (paired Sc)
Hematite
Experiment
Calculation (isolated Sc)
Calculation (paired Sc)
Sc-chloride solution
Sc-adsorbed goethite
Sc-adsorbed hematite
Sc-adsorbed montmorillonite
Fe oxide-rich laterite
Calculation (Oh Sc complex)

Figure 3

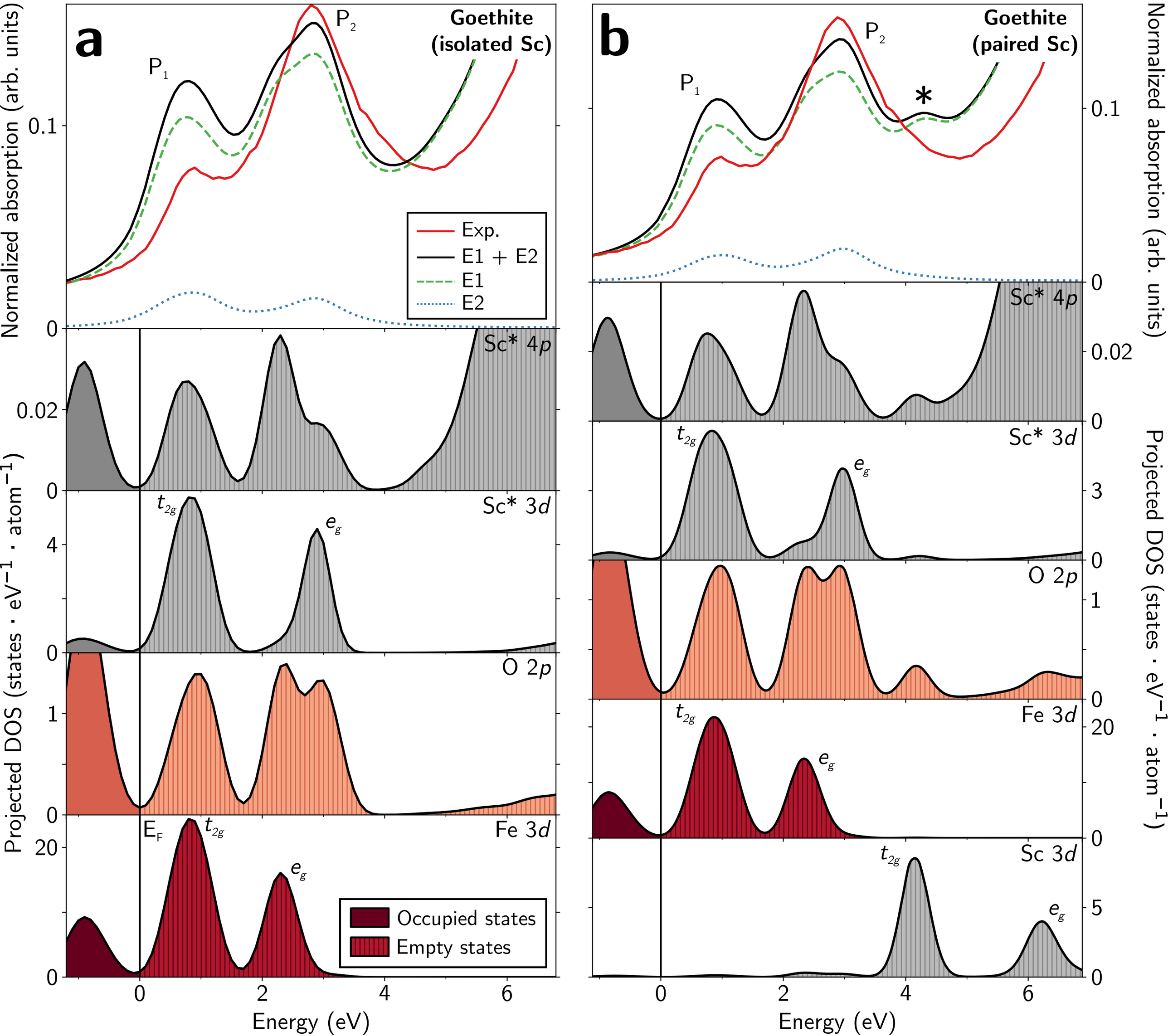
a
Goethite
(isolated Sc)
P1
P2
Exp.
E1 + E2
E1
E2
Sc* 4p
Sc* 3d
t2g
eg
O 2p
Fe 3d
EF
Occupied states
Empty states
b
Goethite
(paired Sc)
*
Sc 3d
Normalized absorption (arb. units)
Projected DOS (states · eV−1 · atom−1)
Energy (eV)